UC Irvine
UC Irvine Previously Published Works

Title

Evolution of ibrutinib resistance in chronic lymphocytic leukemia (CLL)

Permalink

https://escholarship.org/uc/item/8c0565s4

Journal

Proceedings of the National Academy of Sciences of the United States of America, 111(38)

ISSN

0027-8424

Authors

Komarova, Natalia L
Burger, Jan A
Wodarz, Dominik

Publication Date

2014-09-23

DOI

10.1073/pnas.1409362111

Peer reviewed

Evolution of ibrutinib resistance in chronic lymphocytic leukemia (CLL)

Natalia L. Komarova[a,b,1], Jan A. Burger[c], and Dominik Wodarz[a,b]

[a]Department of Mathematics and [b]Department of Ecology and Evolutionary Biology, University of California, Irvine, CA 92697; and [c]Department of Leukemia, MD Anderson Cancer Center, Houston, TX 77230

The Bruton tyrosine kinase inhibitor (BTKi) ibrutinib is a new targeted therapy for patients with chronic lymphocytic leukemia (CLL). Ibrutinib is given orally on a continuous schedule and induces durable remissions in the majority of CLL patients. However, a small proportion of patients initially responds to the BTKi and then develops resistance. Estimating the frequency, timing, and individual risk of developing resistance to ibrutinib, therefore, would be valuable for long-term management of patients. Computational evolutionary models, based on measured kinetic parameters of patients, allow us to approach these questions and to develop a roadmap for personalized prognosis and treatment management. Our kinetic models predict that BTKi-resistant mutants exist before initiation of ibrutinib therapy, although they only comprise a minority of the overall tumor burden. Furthermore, we can estimate the time required for resistant cells to grow to detectable levels. We predict that this can be highly variable, depending mostly on growth and death rates of the individual CLL cell clone. For a specific patient, this time can be predicted with a high degree of certainty. Our model can thus be used to predict for how long ibrutinib can suppress the disease in individual patients. Furthermore, the model can suggest whether prior debulking of the tumor with chemo-immunotherapy can prolong progression-free survival under ibrutinib. Finally, by applying the models to data that document progression during ibrutinib therapy, we estimated that resistant mutants might have a small (<2%) mean fitness advantage in the absence of treatment, compared with sensitive cells.

evolutionary dynamics | drug resistance | personalized medicine | mathematical models | stochastic dynamics

Chronic lymphocytic leukemia (CLL), the most common adult leukemia in the Western hemisphere, is characterized by the expansion of CD5+CD23+ mature monoclonal B cells in the peripheral blood, as well as in lymph nodes and bone marrow. B-cell receptor (BCR) signaling plays a central pathogenic role in CLL, based on structural restrictions of the BCR and BCR-dependent survival and growth of the malignant B cells (1, 2). Bruton tyrosine kinase (BTK), a nonreceptor tyrosine kinase of the Tec kinase family, is essential for BCR signaling. Ibrutinib (previously called PCI-32765) is a potent (IC$_{50}$, 0.5 nM) BTK inhibitor that inactivates BTK through irreversible covalent bonding to Cys-481 in the ATP-binding domain of BTK (3–5). Early-stage clinical trials found ibrutinib to be particularly active in patients with CLL (6, 7) and mantle cell lymphoma (8), and the drug recently has been Food and Drug Administration-approved for patients with relapsed CLL and mantle cell lymphoma.

Preclinical models demonstrated that ibrutinib inhibits CLL cell survival and proliferation (9), as well as leukemia cell migration toward tissue-homing chemokines (CXCL12, CXCL13) and integrin-mediated CLL cell adhesion (10, 11). For patients with CLL, ibrutinib is given orally as a once-daily fixed dose of 420 mg on a continuous schedule until progression or toxicity. In contrast to conventional chemo-immunotherapy, ibrutinib generally is not myelo-suppressive, and responses are not affected by risk factors that predict failure to respond to or short remission durations after chemo-immunotherapy, such as del17p.

In CLL, ibrutinib characteristically causes an early redistribution of tissue-resident CLL cells into the peripheral blood, with rapid resolution of enlarged lymph nodes, along with a surge in lymphocytosis (7, 12). This lymphocytosis is asymptomatic, transient, and resolves in most patients during the first few months of therapy. However, the majority of ibrutinib-treated patients do not achieve complete remission (7), and instead the lymphocyte counts stabilize in the long term in many patients at levels that are significantly lower than before treatment, but higher than normal.

Although the clinical data so far demonstrate extremely encouraging responses in patients, the question arises as to how long the control of the disease can be maintained during continuous ibrutinib therapy. In particular, drug-resistant mutants can arise that can initiate renewed growth. Indeed, in a minority of patients the growth of drug-resistant mutants has already been documented (13–15). Resistance has been found to be caused by point mutations, and a number of different mutants have been documented. These mutants have been shown to have a mutation in the BTK binding site of ibrutinib or gain-of-function mutations in PLCγ2, which lead to autonomous BCR activity. The aim of our study was to determine whether, based on previously measured kinetic parameters of the disease in the absence of treatment (16) and during ibrutinib therapy (17), it is possible to use mathematical models to predict the evolutionary dynamics of ibrutinib-resistant mutants, and to predict how long control of CLL with single-agent ibrutinib treatment can be maintained.

Results

BTK Inhibitor-Resistant CLL Cells Are Present Before the Start of Treatment. An important question that is currently debated in the context of targeted treatments of cancer is whether resistant subclones are present before the start of therapy, or whether they

---

Significance

Chronic ymphocytic leukemia is the most common leukemia, mostly arising in patients over the age of 50. The disease has been treated with chemo-immunotherapies with varying outcomes, depending on the genetic make-up of the tumor cells. Recently, a promising new tyrosine kinase inhibitor, ibrutinib, has been developed, which resulted in successful responses in clinical trials, even for the most aggressive chronic lymphocytic leukemia types. The crucial current questions include how long disease control can be maintained in individual patients, when drug resistance is expected to arise, and what can be done to counter it. Computational evolutionary models, based on measured kinetic parameters of patients, allow us to address these questions and to pave the way toward a personalized prognosis.

evolve during the treatment phase. Here, this question is ana-lyzed in the context of ibrutinib treatment of CLL.

Using our computational modeling approach, we assume that a colony of cancer cells grows stochastically from a single cell, and at each division there is a small probability of creating a re-sistant mutant. In the simplest scenario, we assume that: (*i*) the mutants are neutral in the absence of treatment (that is, they grow at the same rate as the wild-type CLL cells); (*ii*) CLL cells acquire drug-resistant mutations at the physiological mutation rate of human cells, and thus do not display elevated mutation rates (e.g., caused by genetic instability); and (*iii*) mutant gen-eration requires one genetic hit.

Under the scenario just described, Fig. 1 plots the probability of creating at least one resistant mutant for different colony sizes and different mutation rates. The vertical axis shows the $\log_{10}$ col-ony size upon detection, and the horizontal axis shows the range of $\log_{10}$ mutation rates. The numbers marked next to individual con-tours on the graph denote the probability of existence of resistant mutants. For example, we can see that for small mutation rates and for very small colony sizes (the lower left corner of the diagram) the probability of resistance is negligible. This probability grows with the mutation rate and with the colony size.

For CLL, the relevant parameter regime is shown by a rectangle in the upper left part of the diagram in Fig. 1. We assume that the number of CLL cells in tissue upon start of treatment ranges be-tween 10^{12} and 10^{13} (as demonstrated in ref. 17). The range of possible mutation rates is taken between 10^{-9} and 10^{-7}. If resistance can only be induced by a single point mutation, then the mutation rate would be 10^{-9} (18–22). In contrast, if multiple different point mutations can independently induce resistance, then the mutation rate is higher. It is reasonable to assume an upper limit for the mutation rate of 10^{-7}, which means that hundreds of different point mutations can independently cause resistance. As we can see, for this region of the diagram in Fig. 1, the probability of resistance gener-ation is very close to 1. Calculations show that this probability is always greater than 0.995; in other words, the chance of not finding resistance is smaller than 0.5%. This lowest bound corresponds to the colony size of 10^{12} and the mutation rate of 10^{-9}. We note that this finding holds true for any division and death rates. We have il-lustrated our cases assuming that the death rate is 10% of the di-vision rate. The lowest chance to generate resistance during growth occurs when the expanding cell population does not die (23). Even

under this extreme assumption, the probability that resistant mutants exist upon treatment initiation is still practically certainty.

Now, suppose that assumption (*i*) above does not hold. In the next section we present indication that ibrutininb-resistant CLL cells may have a certain fitness advantage, even in the absence of treatment. In this case, our conclusions definitely hold, and the presence of resistance before treatment is a certainty. Next, let us assume that resistant mutants are characterized by a certain se-lective disadvantage compared with wild-type [although this has not been observed for ibrutinib treatment of CLL, it has been observed in the context of other targeted cancer therapies (24)]. In this case, it turns out that the estimates for the probability of resistance are very nearly the same as shown above. Regardless of the properties of the mutants, the probability of mutant generation is extremely high. The reason that it does not depend on whether the mutants are advantageous or disadvantageous is because the main contribution to mutant generation comes from a very large (compared with the inverse mutation rate) number of cell divisions. In other words, it is most likely that the resistant mutants are generated relatively late in the colony's history, where the population is so large that a new mutant is very likely to be produced in each generation. This finding is in contrast to another possible mechanism whereby a mutant is generated early in the colony's history and grows to large numbers. The latter scenario, which is strongly dependent on the mutant properties of growth, does not contribute significantly here.

If assumption (*ii*) above does not hold, that is, if ibrutinib-resistant mutants are generated with an elevated mutation rate, the chances of having resistance are even higher. In other words, this assumption does not influence our conclusion.

The only circumstance under which we can expect the pres-ence of resistance with less certainty is if assumption (*iii*) is violated; that is, if mutant generation requires more than one mutational hit (for example, if gene amplification is required for resistance) (25). The higher the number of mutational steps required, the less the chance of generating a resistant cell by the time of detection. Be-cause the only documented ibrutinib-resistant mutants have been shown to be caused by point mutations, however, we will focus on this scenario (14, 15).

Resistant Mutants Can Have a Selective Advantage in the Absence of Treatment. We know that resistant mutants enjoy a significant advantage during treatment as they continue to grow, whereas wild-type cells decline under ibrutinib. What can we say about growth properties of mutants in the absence of treatment? For PLCgγ2 mutations, calcium flux in DT40 cells after stimulation with anti-IgM antibody was enhanced compared with nonmutant PLCgγ2, even in the absence of ibrutinib (15). This result indicates enhanced pathway activation in the context of the PLCgγ2 mutation, which could theoretically translate into a survival and fitness advantage of mutant cells, although this has so far not been demonstrated. For the mutation in the ibrutinib-binding site in BTK, there is so far no indication for a mutant fitness advantage (15).

These data cannot tell us whether resistant mutants indeed enjoy a fitness advantage compared with the wild-type when they grow in vivo in the absence of treatment. Therefore, we will use an epidemiological approach to investigate this question. In par-ticular, we will use the data collected so far on ibrutinib treatment response in CLL patients to see what level of mutant fitness is consistent with the observations. Using the literature, we compiled the information on nine different cohorts of CLL patients who were treated with ibrutibib for different median time durations (6, 7, 13, 26–29) (see *SI Appendix* for details). The number of patients showing progressive disease was reported in each case. Using computer simulations, we determined what level of mutant fitness in the absence of treatment is most consistent with these data. Al-though the exact numbers depend somewhat on the assumed level of mutant detection (*SI Appendix*), one overall conclusion is clear: if the resistant mutants have a fitness advantage in the absence of treatment, this advantage is not very large, about 1.5%. This figure refers to the mean fitness advantage. In other words, if all resistant

Fig. 1. Probability of resistance generation. The horizontal axis is the $\log_{10}$ of the mutation rate, and the vertical axis is the $\log_{10}$ of the colony size at de-tection. Because these two parameters vary within many orders-of-magnitude, we calculated the probability of resistance generation. The latter is presented as a contour plot, where the contours (with the values marked next to them) represent constant-level sets of probability. The black rectangle in the upper left corner represents the parameter values relevant for CLL. The division and death parameters for wild-type and mutant cells are given by $l_w = l_r = 1$ and $d_w = d_r = 0.1$. The results do not change visibly if we take $l_w = l_r = 1$, $d_w = d_r = 0$.

mutants have the same fitness in the absence of treatment, then this fitness is 1.5% larger than that of the wild-type. If, on the other hand, only 10% of all ibrutinib-resistant mutations confer fitness advantage and the rest 90% are neutral in the absence of treatment, then the advantageous mutants must be about 15% fitter than the wild-type, thus yielding the same 1.5% mean fitness advantage.

The Number of Resistant Cells at Detection Is Very Low. By using our model, we were able to predict the expected population size of resistant cells at the time of tumor detection. Using the parameter values from Messmer et al. (16) and Wodarz et al. (17), we find that the number of mutants in patients at the start of treatment typically has the order-of-magnitude of 10^6 to 10^8 cells. In Fig. 2*A* we present a histogram of numerically predicted mutant population sizes that were obtained in the following way. We randomly picked division and death rates chosen inside the bounds given by Messmer et al. (16) and paired them with randomly selected population sizes at treatment start chosen between the minimum and the maximum values measured in Wodarz et al. (17). A population of 1,000 artificial "patients" was created in this way, and then the expected number of mutants at start of treatment was calculated. We performed this procedure assuming that resistant mutants are neutral at the start of treatment (the blue histogram in Fig. 2*A*), and then repeated it with the assumption that resistant mutants have a 1.5% fitness advantage in the absence of treatment (the red histogram Fig. 2*A*). We can see that the median values for the mutant population are very similar in the two cases (and given by 1.1×10^7 and 1.9×10^7 cells). The main difference manifests itself in a thicker "tail" of the distribution: if the mutants have a selective advantage before treatment, there will be a very small percentage of patients with a significant population of resistant mutants at the start of treatment. About 0.1% of the artificial "patients" had a population of mutants greater than 1% of the total CLL cells.

The question arises as to whether these mutants can be responsible for the long-term dynamics of CLL cells observed during a time period of 2–3 y. The majority of the patients treated with ibrutinib do not achieve complete remission. At present, the reason for the corresponding long-term stabilization of the lymphocyte counts is unknown. One hypothesis could be that it arises from resistant cells that are generated in the colony. Because these cells do not respond to treatment, they could be the ones that remain after prolonged treatment.

To test this hypothesis we need to compare the predicted sizes of the mutant colonies with the number of CLL cells in tissue during the plateau phase. The number of CLL cells in the blood has been measured during this time frame, but the great majority of the disease resides in the tissue. Based on the blood measurements and on volumetric analysis in the tissue, the number of CLL cells in the tissue has been estimated in ref. 17. During the plateau phase, the obtained values of CLL cells in tissue were

rather varied, with the median of 1.25×10^{11} and the minimum value given by 4×10^8.

Our computations show that the presence of resistant mutants in CLL is unlikely to explain the long-term stabilization of the lymphocyte counts in the patients. In Fig. 2*B* we present a histogram of projected mutant population sizes after 300 d of treatment. We can see that the majority of patients will have a mutant colony sizes that are about 10^3-times smaller than the typical plateau value for CLL cells. The median size of a mutant colony after 300 d is 4.0×10^7 and 9.7×10^7 cells, for neutral and advantageous (1.5%) mutants, respectively. This number is much smaller than the median of 1.25×10^{11} for estimated numbers of tissue CLL cells during the plateau phase. Another reason for the observed plateau to be of a different nature compared with a resistant clone is that the former is relatively stable, whereas the latter is predicted to expand exponentially, and can thus show different overall dynamics, depending on the rate at which resistant mutants grow.

To conclude, our analysis shows that at the time of treatment initiation, and even after 300 d of treatment with ibrutinib, resistant mutant colonies are most likely to be very small, well below the detection limit. This finding is in agreement with the currently available data (14, 15). Resistance mutations were detected when progressive disease was first observed, but not before treatment or during the initial response to treatment (including lymphocytosis) (14, 15). In addition, the CLL cells found during lymphocytosis in nonprogressing patients have been found to be quiescent rather than carrying mutations that confer ibrutinib resistance (30, 31).

When Can Resistance Be Detected? We have shown that typically, we do not expect resistance to be observable for the time frames of treatment considered so far (300 d after therapy initiation). It is inevitable, however, that the resistant colony will grow and eventually become sizable. The question is how long this process may take.

We have run the mean course of resistant-mutant growth starting from the expected mutant numbers at the start of treatment. We assume that resistance becomes a problem and contributes to visible disease relapse when the size of the resistant colony reaches 10^{10} cells. Although we know the number of tumor cells in the blood at which the disease becomes detectable, most of the CLL cells reside in tissue. The population size threshold for detection of solid tumors is about 10^9 cells (32), and for the CLL cells to accumulate at detectable levels in the blood, the tissue disease burden likely has to be larger, hence our threshold level of 10^{10} cells.

As before, we studied 1,000 parameter combinations randomly created using the bounds from Messmer et al. (16) and Wodarz et al. (17). Assuming the mutation rate of 10^{-8}, the model shows that 6% (12%) of patients in our sample will develop resistance before 2 y after start of treatment, 46% (59%) of patients will develop resistance before 5 y, and 75% (86%) of patients will develop it before 10 y (the amount in parenthesis refers to resistant mutants having an average fitness advantage of 1.5%). For 5% (1%) of the patients, resistance will not come up for the first 30 y after treatment. The mean time of developing resistance is about 9 y (5) after start of treatment. A numerical probability distribution function for the time when resistance reaches detection level is presented in Fig. 3.

Despite the fact that resistance is present with certainty in all tumors upon detection, the dynamics of resistance growth is predicted to be very different for different patients. Without assuming any differences in the mechanisms of resistance, the only parameters that are varied across our set are (*i*) the size of tumor at start of treatment and (*ii*) the kinetic parameters of untreated CLL cells. It turns out that it is the net growth rate of mutants (parameter $l_m - d_m$; i.e., division minus death rate of cells) that defines the eventual fate of the treatment. Fig. 4 illustrates this statement. In Fig. 4*A* and *B* we plot the expected growth dynamics of mutant colonies for neutral mutants and mutants with a 1.5% fitness advantage before treatment, respectively. The most noticeable difference between the two cases is that slightly advantageous mutants are present above the detection level in a small percentage of patients at the start of treatment. In both
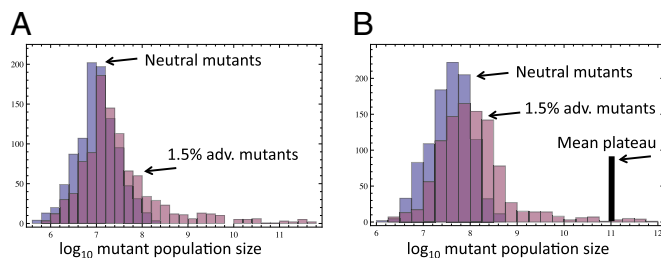
Fig. 2. A histogram of mutant population sizes: (*A*) at start of treatment and (*B*) after 300 d of treatment. Plotted are results for a population of 1,000 artificial "patients" (with parameters from refs. 16 and 17). Blue histograms correspond to the assumption that resistant mutants are neutral and red, that they have a 1.5% fitness advantage in the absence of treatment. The vertical bar in *B* marks the mean value of the plateau of CLL cells achieved upon treatment in ref. 17. The mutation rate is 10^{-8}.

graphs we observe a wide range of dynamic behaviors, where in some patients resistance does not arise before 10 y, and in others it comes up very quickly. What parameter is mostly responsible for this difference? Mathematically, the time to resistance for each patient decays with the mutant growth rate and with the tumor burden at start of treatment. The former parameter, however, exhibits an overall stronger influence on the rise of resistance. In Fig. 4C we plot, for each patient, the inverse time it takes for mutants to rise above the detection level of 10^{10} cells as a function of the net growth rate of the cells. We can see a strong positive correlation. The much weaker dependence on the population size at the start of treatment is masked by the growth rate correlation, as shown in Fig. 4D.

We conclude that the measured difference in the net growth rates of CLL cells alone (without evoking the differences in the mechanisms of resistance) can give rise to a significant heterogeneity of resistance growth dynamics. Furthermore, it is the net growth rates of CLL, rather than the size of the tumor upon initiation of therapy, which are predicted to be the strongest correlates of resistance.

Average Behavior and Stochastic Variations. So far, our results on the dynamics of mutant growth are based on averages derived from deterministic models. We have observed significant heterogeneity in the average time until resistant mutants grow to significant levels, based on differences in the parameters by which the patients are characterized, most importantly the rate of cell division and the rate of cell death. However, even if these parameters are identical, variation in the time until resistance rises to higher levels can come about through stochasticity that is inherent in the dynamics of cell growth, especially during phases when mutants grow from low numbers. Therefore, we performed numerical analysis of the stochastic model to study the variance in outcomes (*SI Appendix*).

Two measures were considered: (*i*) The number of mutants when treatment was initiated. Treatment was assumed to start when the number of tumor cells reached 8×10^{12}, which is the average estimated tumor size at the start of ibrutinib treatment in our previous study (17). (*ii*) The time it takes for the resistant mutant to grow to significant levels. In these computations, we defined the time when the number of resistant tumor cells in the tissue compartments reached 10^9 cells.

The algorithm was used for two parameter combinations, one characterized by faster growth (slow turnover of cells, where division rate of cells is much larger than death rate), and one characterized by slower growth (fast turnover, where division rate of cells is close to death rate). The results are similar for both scenarios and shown in Fig. 5. First consider the number of cells at start of therapy (Fig. 5A). We can see that there is a large degree of variation in this number, with a SD that is an order-of-magnitude higher than the mean (please note the logarithmic scale on the horizontal axis). This phenomenon has been previously described (33). On the other hand, the time until the resistant mutant reaches the threshold population size shows a much more narrow distribution and only little variation (Fig. 5 *B* and *C*). The SD for
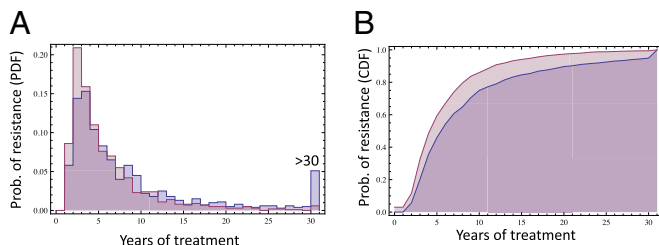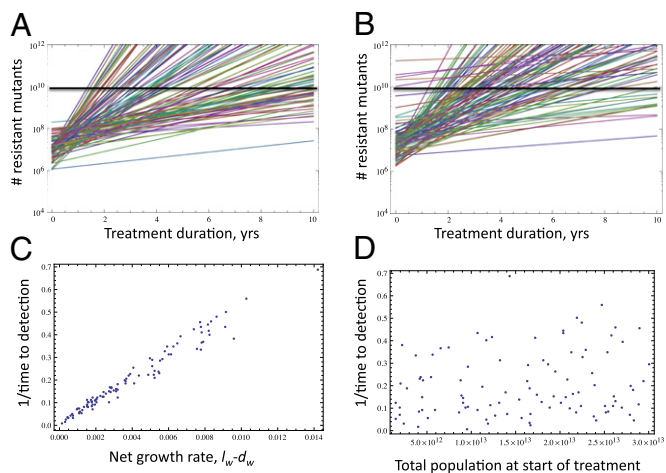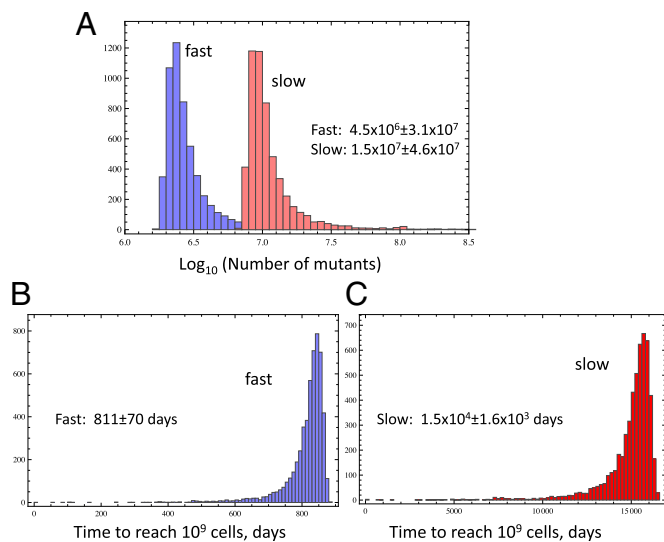
Fig. 4. The growth dynamics of resistant mutants. (*A* and *B*) The mean growth dynamics of mutants calculated for 100 parameter combinations, created as in Fig. 2. The mutation rate is 10^{-8}. The detection threshold of 10^{10} cells is marked by a horizontal line. In *A*, the resistant mutants are neutral in the absence of treatment, and in *B* they have a fitness advantage of 1.5%. (*C*) The inverse time of mutant detection is plotted against the net growth rate, $l_w - d_w$ for all of the "patients" in *A*. (*D*) Same as in *C*, but plotted against the tumor size at the start of treatment. In panels *C* and *D* we assume that the mutants are neutral in the absence of treatment.

the timing of mutant growth is an order-of-magnitude lower than the mean. The reason is that the time until the resistant mutant population rises to a threshold size is determined by the logarithm of the mutant population size at the start of treatment (*SI Appendix*), which logarithmically reduces the spread in the results.

The insight that there is only a small amount of stochastic variation in the time until the resistant mutant reaches its threshold size for a given parameter set has important practical implications: it enables us to predict the long-term treatment outcome with ibrutinib, and to tailor treatment strategies individually to avoid complications from resistance. The time until resistant mutants emerge to significant levels is rather accurately predicted by the average. Hence, measurements of the cell division and death rates by heavy water labeling, and estimations of total tissue tumor burden from radiological data, can enable us to predict for how long continuous ibrutinib treatment can control CLL. If control is predicted to be maintained for decades, no special strategies to combat resistance are likely needed. In contrast, if tumor relapse because of resistance is predicted to occur within a few months, treatment schedules will have to be designed to prevent this relapse, as described next.

Strategies to Overcome Resistance. The above analysis indicates that drug-resistant mutants arise during the growth phase of CLL before the onset of treatment, and continue to grow during treatment. If resistant cells grow sufficiently to contribute to relapse during the life span of the patient, measures have to be implemented to combat this resistance against ibrutinib.

The first question to examine is whether early treatment, immediately upon detection, would significantly lower the probability that resistant mutants exist at the start of therapy. Let us assume that resistance is generated with a mutation rate of 10^{-8} and that the lowest detectable tumor tissue burden is approximately 10^9 cells. Fig. 6A shows the probability that mutants resistant against ibrutinib exist as a function of the tissue tumor burden. This is plotted for different tumor cell turnover rates [i.e., ratios of cell division and death, as estimated in Messmer et al. (16)]. Fig. 6A shows that once the number of tissue tumor cells rises beyond 10^9 cells, the probability for resistant mutants to exist is very high, about 93% for the lowest turnover rates and higher values for higher turnover rates. This finding is also shown in Fig. 6B. In this figure, we assumed that resistant mutants do not have a fitness advantage in the absence of

Fig. 3. Numerically obtained probability distribution function for the expected time when a resistant colony reaches detection level, for different combinations of kinetic parameters. The artificial patient population of 1,000 was created as in Fig. 2; the mutation rate is 10^{-8}. (*A*) The probability density function. (*B*) The cumulative distribution function.

EVOLUTION

Fig. 5. Stochasticity of mutant dynamics. (*A*) Histograms of the simulated number of mutants at the start of treatment (when the colony reaches size 8×10^{12}). (*B* and *C*) The histograms of the time it takes for the mutant colony to reach the detection level of 10^9 cells. Two parameter combinations have been simulated: "slow" ($l_w = l_r = 0.0029$, $d_w = d_r = 0.0026$) and "fast" ($l_w = l_r = 0.0178$, $d_w = d_r = 0.0106$). The total number of simulations is about 5,000 for each parameter set. The mutation rate is assumed to be 10^{-8}. For each measurement, for "fast" and "slow" parameters, the mean ± SD is indicated.

treatment. If we assume a fitness advantage, this result becomes even stronger. Once the number of tumor cells has risen to 10^{10}, they exist with certainty, irrespective of the turnover rate of the tumor in the patient. Because the disease is not likely to be detectable at tissue population sizes that are less than 10^9 cells, an early start of ibrutinib treatment is unlikely to significantly improve the duration for which the drug can control the tumor.

Another strategy to combat resistance could be to first debulk the tumor with chemo-immunotherapy, followed by treatment with ibrutinib. This could improve outcome in two ways.

First, although resistance is very likely to be present when the disease becomes detectable in blood, the probability that resistant mutants are present is lower if the disease burden is pushed to lower levels. In some patients, chemo-immuotherapy can reduce the number of CLL cells below detection in blood. Let us assume that in tissue the number of cells is reduced to 10^8. In this case, resistant mutants are present in about 50% of patients if the turnover rate of the tumor is low (Fig. 6 *A* and *B*). Thus, debulking could pave the way for resistance-free ibrutinib treatment in about half of the patients. For high turnover tumors, however, this would not apply because the probability for resistant mutants to be present at 10^8 cells is much higher (Fig. 6 *A* and *B*). Elimination of the ibrutinib-resistant mutants further requires that no mutants are present that are simultaneously resistant against ibrutinib and chemo-immunotherapy. In the worst-case scenario, resistance against chemo-immunotherapy is also acquired by a single mutation. In this case, Fig. 6*C* shows that upon initiation of treatment [when tissue disease burden is at 8×10^{12} (17)], the chances of having doubly resistant mutants are relatively low (10–20%) for low-turnover tumors, but much higher if the turnover rate is large (see also Fig. 6*B*). These plots are based on a mutation rate of 10^{-8} per cell division and neutral resistant mutants. The probabilities would be less for lower mutation rates, but higher for resistant mutants that have a fitness advantage in the absence of treatment. Thus, elimination of ibrutinib-resistant mutants by prior debulking is difficult to achieve and can only have a chance to be successful for low-turnover tumors.

Second, even if resistance is still present after debulking, the number of mutants is going to be significantly lower than before

debulking, which could lead to a longer duration for which the patient remains progression-free during ibrutinib therapy (Fig. 6*D*). Assume that chemo-immunotherapy reduces the tumor burden by two orders-of-magnitude. For the same parameters as above, the average time until progression now increases from 9 to 12.8 y. Fewer than 1% of patients (rather than 6%) are predicted to progress in <2 y, 24% (rather than 46%) in <5 y, 55% (rather than 75%) in <10 y, and 14% (rather than 5%) of patients are predicted to remain progression-free for >30 y.

A currently more hypothetical strategy could be to combine different kinase inhibitors [such as idelalisib (34)] with ibrutinib to prevent resistance-induced disease progression. If mutations that confer resistance against ibrutinib do not simultaneously confer resistance to the other inhibitors, then Fig. 6*C* shows that for low-turnover treatment, the probability for two-drug resistance is relatively low, and hence a combination of two drugs could work. This is, however, not the case for high-turnover rates. For such tumors, more drugs would have to be combined to prevent resistance-induced disease progression. This theory can be explored further mathematically with the framework provided by Komarova and Wodarz (23), although it remains to be explored whether such combination treatments would be clinically practical considering the side effects.

Discussion

We used previously estimated key parameters of CLL dynamics in the absence of treatment and in the presence of ibrutinib therapy, as well as patient follow-up data, to analyze the evolutionary dynamics of drug resistant cell clones. The following key insights were obtained by using methods of evolutionary and computational biology:

First, drug-resistant CLL cells are almost certain to exist by the time of ibrutinib treatment initiation. Therefore, it is the pre-existence of resistant cells that is important. The treatment phase
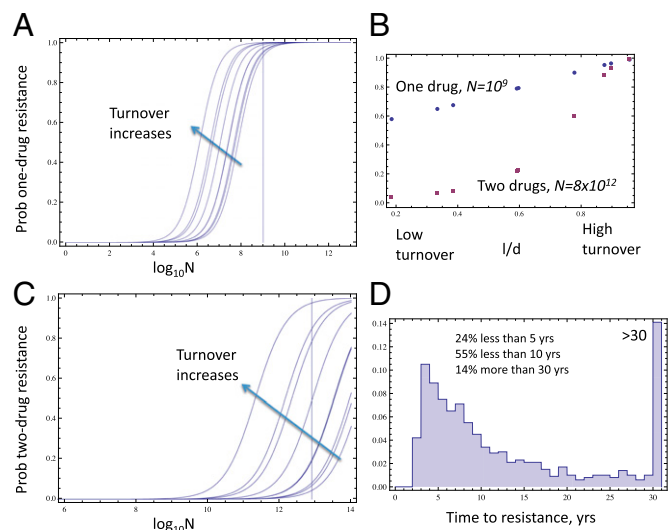
Fig. 6. Dynamics of resistance. (*A*) The probability of one-drug resistance to be generated in a colony of CLL cells before treatment, as a function of the population size. The different lines correspond to different values of the cellular turnover, d_w/l_w, taken from the nine sets of parameters in ref. 16. The vertical line marks the detection size, 10^9 cells. (*B*) Circles: The probability of one-drug resistance for different values of the turnover (horizontal axis) at size $n = 10^9$. Squares: The probability of two-drug resistance for different values of the turnover at size $n = 8 \times 10^{12}$. (*C*) Same as in *A*, but for the probability of two-drug resistance. The vertical line marks the mean treatment size in ref. 16, 8×10^{12}. (*D*) Numerically obtained probability distribution function for the expected time when a resistant colony reaches level 10^{10}, after reducing the tumor size by a factor of 0.01 by debulking (compare with Fig. 3*A* in the absence of debulking). The mutation rate is 10^{-8}.

Komarova et al.

is unlikely to contribute significantly to resistance generation. Hence, the dynamics that are observed during ibrutinib treatment, including the lymphocytosis phase, are not likely to contribute to the evolution of resistant mutants.

Second, drug-resistant mutants are unlikely to explain the lack of complete remission during ibrutinib therapy. The predicted number of resistant cells during this phase is too low to account for the observed plateau to which the CLL cell population converges during treatment.

Third, the time until resistant mutants grow to sufficient levels to contribute visibly to disease relapse is predicted to vary extensively across patients because of known variations in the basic parameters describing the rate of clonal expansion. This in turn defines the rate at which drug resistant CLL cells divide and die in tissue during drug therapy. In general, we predict that significant interpatient variations in resistance dynamics will be caused by genetic differences in the tumors alone. Further variations can be caused by other factors, such as genetic differences among the patients and the specific types of resistance mutations acquired.

Fourth, although differences in cellular growth parameters across patients can lead to extensive variation in the time until visible relapse occurs, for a given set of parameters, stochastic variation in outcome is limited. Therefore, the expected time until disease relapse is a reliable indicator for how long ibrutinib monotherapy can control the disease for a particular patient.

Finally, depending on the relative rates of CLL cell division and cell death, it might be possible to increase the duration of progression-free survival during ibrutinib treatment by debulking the tumor with chemo-immmunotherapy before ibrutinib therapy.

These insights open up the possibility to use such computational models for personalized predictions about the outcome of treatment. For each patient, the division and death rate of cells should be measured with heavy water labeling, and the tissue tumor load before treatment initiation should be estimated with CT scans. Based on these measures, we can predict the average duration for which ibrutinib monotherapy can maintain control of the disease, when resistance is likely to emerge, and whether specific measures to prevent relapse are likely to be helpful.

Besides predictions about the dynamics of disease relapse, another important contribution of our calculations is that we were able to provide a first estimate of resistant-mutant fitness. This estimate will need to be refined when more clinical data become available that document the timing of disease relapse during ibrutinib treatment. The methodology presented here is indirect, and infers mutant fitness from epidemiological data; this is akin to similar approaches that have been used to infer in vivo processes from epidemiological data in cancer research (35–37). It is likely one of the more reliable ways to estimate mutant fitness. Although a direct measurement would obviously be preferable, this might be very difficult to achieve. The growth properties of CLL cells depend intricately on the tissue microenvironment in humans, which renders any experimentation and direct approaches challenging.

Materials and Methods

We use methods of evolutionary and computational biology to answer questions about the evolutionary dynamics of BTK inhibitor resistance in CLL. Deterministic and stochastic methods are used. Please see *SI Appendix* and refs. 38 and 39 for complete details.

1. Burger JA, Chiorazzi N (2013) B cell receptor signaling in chronic lymphocytic leukemia. *Trends Immunol* 34(12):592–601.
2. Chiorazzi N, Rai KR, Ferrarini M (2005) Chronic lymphocytic leukemia. *N Engl J Med* 352(8):804–815.
3. Pan Z, et al. (2007) Discovery of selective irreversible inhibitors for Bruton's tyrosine kinase. *ChemMedChem* 2(1):58–61.
4. Honigberg LA, et al. (2010) The Bruton tyrosine kinase inhibitor PCI-32765 blocks B-cell activation and is efficacious in models of autoimmune disease and B-cell malignancy. *Proc Natl Acad Sci USA* 107(29):13075–13080.
5. Burger JA, Buggy JJ (2013) Bruton tyrosine kinase inhibitor ibrutinib (PCI-32765). *Leuk Lymphoma* 54(11):2385–2391.
6. Advani RH, et al. (2013) Bruton tyrosine kinase inhibitor ibrutinib (PCI-32765) has significant activity in patients with relapsed/refractory B-cell malignancies. *J Clin Oncol* 31(1):88–94.
7. Byrd JC, et al. (2013) Targeting BTK with ibrutinib in relapsed chronic lymphocytic leukemia. *N Engl J Med* 369(1):32–42.
8. Wang ML, et al. (2013) Targeting BTK with ibrutinib in relapsed or refractory mantle-cell lymphoma. *N Engl J Med* 369(6):507–516.
9. Herman SE, et al. (2011) Bruton's tyrosine kinase represents a promising therapeutic target for treatment of chronic lymphocytic leukemia and is effectively targeted by PCI-32765. *Blood* 117(23):6287–6296.
10. Ponader S, et al. (2012) The Bruton tyrosine kinase inhibitor PCI-32765 thwarts chronic lymphocytic leukemia cell survival and tissue homing in vitro and in vivo. *Blood* 119(5):1182–1189.
11. de Rooij MF, et al. (2012) The clinically active BTK inhibitor PCI-32765 targets B-cell receptor- and chemokine-controlled adhesion and migration in chronic lymphocytic leukemia. *Blood* 119(11):2590–2594.
12. Burger JA, Buggy JJ (2013) Bruton tyrosine kinase inhibitor ibrutinib (PCI-32765). *Leuk Lymphoma* 54(11):2385–2391.
13. Chang BY, et al. (2013) Use of tumor genomic profiling to reveal mechanisms of resistance to the BTK inhibitor ibrutinib in chronic lymphocytic leukemia (CLL). *2013 ASCO Meeting Abstracts*, Abstract no. 7014.
14. Furman RR, et al. (2014) Ibrutinib resistance in chronic lymphocytic leukemia. *N Engl J Med* 370(24):2352–2354.
15. Woyach JA, et al. (2014) Resistance mechanisms for the Bruton's tyrosine kinase inhibitor ibrutinib. *N Engl J Med* 370(24):2286–2294.
16. Messmer BT, et al. (2005) In vivo measurements document the dynamic cellular kinetics of chronic lymphocytic leukemia B cells. *J Clin Invest* 115(3):755–764.
17. Wodarz D, et al. (2014) Kinetics of CLL cells in tissues and blood during therapy with the BTK inhibitor ibrutinib. *Blood* 123(26):4132–4135.
18. Alberts B, et al. (2013) *Essential Cell Biology* (Garland Science, New York).
19. Calabrese P, Shibata D (2010) A simple algebraic cancer equation: Calculating how cancers may arise with normal mutation rates. *BMC Cancer* 10:3.
20. Sverdlov ED, Mineev K (2013) Mutation rate in stem cells: An underestimated barrier on the way to therapy. *Trends Mol Med* 19(5):273–280.
21. Tomlinson I, Sasieni P, Bodmer W (2002) How many mutations in a cancer? *Am J Pathol* 160(3):755–758.
22. Tomlinson IP (2001) Mutations in normal breast tissue and breast tumours. *Breast Cancer Res* 3(5):299–303.
23. Komarova NL, Wodarz D (2005) Drug resistance in cancer: Principles of emergence and prevention. *Proc Natl Acad Sci USA* 102(27):9714–9719.
24. Tipping AJ, Mahon FX, Lagarde V, Goldman JM, Melo JV (2001) Restoration of sensitivity to STI571 in STI571-resistant chronic myeloid leukemia cells. *Blood* 98(13):3864–3867.
25. Gorre ME, et al. (2001) Clinical resistance to STI-571 cancer therapy caused by BCR-ABL gene mutation or amplification. *Science* 293(5531):876–880.
26. Byrd JC, et al.; RESONATE Investigators (2014) Ibrutinib versus ofatumumab in previously treated chronic lymphoid leukemia. *N Engl J Med* 371(3):213–223.
27. Byrd JC, et al. (2012) The Bruton's tyrosine kinase (BTK) inhibitor ibrutinib (PCI-32765) promotes high response rate, durable remissions, and is tolerable in treatment naive (TN) and relapsed or refractory (RR) chronic lymphocytic leukemia (CLL) or small lymphocytic lymphoma (SLL) patients including patients with high-risk (HR) disease: New and updated results of 116 patients in a phase Ib/II study. *54th Annual ASH Meeting and Exposition*, no. 189.
28. O'Brien S, et al. (2014) Ibrutinib as initial therapy for elderly patients with chronic lymphocytic leukaemia or small lymphocytic lymphoma: an open-label, multicentre, phase 1b/2 trial. *Lancet Oncol* 15(1):48–58.
29. Woyach JA, et al. (2014) Association of disease progression on ibrutinib therapy with the acquisition of resistance mutations: A single-center experience of 267 patients. *J Clin Oncol* 32:5s (suppl; abstr 7010).
30. Rossi D, Gaidano G (2014) Lymphocytosis and ibrutinib treatment of CLL. *Blood* 123(12):1772–1774.
31. Woyach JA, et al. (2014) Prolonged lymphocytosis during ibrutinib therapy is associated with distinct molecular characteristics and does not indicate a suboptimal response to therapy. *Blood* 123(12):1810–1817.
32. Del Monte U (2009) Does the cell number 10(9) still really fit one gram of tumor tissue? *Cell Cycle* 8(3):505–506.
33. Komarova NL, Wu L, Baldi P (2007) The fixed-size Luria-Delbruck model with a non-zero death rate. *Math Biosci* 210(1):253–290.
34. Furman RR, et al. (2014) Idelalisib and rituximab in relapsed chronic lymphocytic leukemia. *N Engl J Med* 370(11):997–1007.
35. Luebeck EG, Moolgavkar SH (2002) Multistage carcinogenesis and the incidence of colorectal cancer. *Proc Natl Acad Sci USA* 99(23):15095–15100.
36. Rodriguez-Brenes IA, Komarova NL, Wodarz D (2013) Tumor growth dynamics: Insights into evolutionary processes. *Trends Ecol Evol* 28(10):597–604.
37. Frank SA (2007) *Dynamics of Cancer: Incidence, Inheritance, and Evolution* (Princeton Univ Press, Princeton, NJ).
38. Komarova NL, Wodarz D (2013) *Trageted Treatment in Silico: Small Molecule Inhibitors and ONcolytic Viruses* (Birkhäuser, New York).
39. Wodarz D, Komarova NL (2014) *Dynamics of Cancer: Mathematical Foundations of Oncology* (World Scientific Publishing, London).

EVOLUTION